

## Ferromagnetism at the surface of a LaCoO<sub>3</sub> single crystal observed using scanning SQUID microscopy

A. Harada,<sup>1</sup> T. Taniyama,<sup>1</sup> Y. Takeuchi,<sup>2</sup> T. Sato,<sup>2</sup> T. Kyômen,<sup>3</sup> and M. Itoh<sup>1,\*</sup>

<sup>1</sup>*Materials and Structures Laboratory, Tokyo Institute of Technology, 4259 Nagatsuta, Midori-ku, Yokohama 226-8503, Japan*

<sup>2</sup>*Department of Applied Physics and Physico-Informatics, Faculty of Science and Technology, Keio University, 3-14-1 Hiyoshi, Kohoku-ku, Yokohama 223-8522, Japan*

<sup>3</sup>*Department of Material Engineering, Faculty of Engineering, Gunma University, 1-5-1 Tenjin, Kiryu, Gunma 376-8515, Japan*

(Received 11 January 2007; revised manuscript received 30 March 2007; published 21 May 2007)

Evidence for ferromagnetism at the surface of a LaCoO<sub>3</sub> single crystal is reported using a scanning superconducting quantum interference device (SQUID) microscope. Stray magnetic flux detected with the scanning SQUID shows typical ferromagnetic behavior in LaCoO<sub>3</sub> below  $T_c \sim 85$  K, in agreement with previous work on LaCoO<sub>3</sub> particles. Analysis of the magnetization of LaCoO<sub>3</sub> particle samples clearly shows that the magnetization is inversely proportional to the particle radius, giving the information that the ferromagnetism is restricted within a few unit cell layers from the surface. X-ray photoemission spectroscopy also indicates that the ferromagnetism likely originates from the metallic surface due to hole doping with oxygen chemisorption.

DOI: [10.1103/PhysRevB.75.184426](https://doi.org/10.1103/PhysRevB.75.184426)

PACS number(s): 75.70.Rf, 75.30.Cr, 75.50.Tt, 75.60.-d

Surface magnetism of materials that originally exhibit paramagnetic behavior in bulk has attracted much interest, and a number of studies are reported from both fundamental and engineering viewpoints, with a view to developing spin electronic devices. Recent experimental studies have revealed that  $4d$  transition metals such as Ru, Rh, and Pd show an enhanced Pauli paramagnetic susceptibility and even ferromagnetism at the two-dimensional surface, arising from the high density of states at the Fermi energy.<sup>1-3</sup> Intriguing magnetic enhancement has also been reported in LaCoO<sub>3</sub> powder and nanoparticles. LaCoO<sub>3</sub> bulk has a rhombohedrally distorted perovskite structure and the ground state of the Co<sup>3+</sup> ( $d^6$ ) ion in LaCoO<sub>3</sub> is believed to be the low-spin (LS) state ( $t_{2g}^6 e_g^0$ ). The spins are thermally excited with increasing temperature, and a high-spin (HS) state ( $t_{2g}^4 e_g^2$ ) or an intermediate-spin (IS) state ( $t_{2g}^5 e_g^1$ ) is established near 100 K.<sup>4-8</sup> The spin state transition has its origin in the competition between the crystal field energy ( $\Delta_{cr}$ ) at Co<sup>3+</sup> sites due to the surrounding O<sup>2-</sup> ions and the exchange coupling energy ( $\Delta_{ex}$ ), both of which are almost the same in magnitude.<sup>4</sup> In spite of the nonmagnetic LS ground state, a sharp increase in the magnetic susceptibility of LaCoO<sub>3</sub> powders was observed below 35 K, reminiscent of the ferromagnetism in  $4d$  transition metals in a confined geometry. Richter *et al.* performed ultraviolet photoemission spectroscopy (UPS), x-ray photoemission spectroscopy (XPS), and electron energy-loss spectroscopy measurements and demonstrated that the surface of LaCoO<sub>3</sub> shows an electronic structure which is completely different from that of its bulk due to the absorption of oxygen on the surface.<sup>9</sup> Señarís-Rodríguez *et al.* reported that the HS state of Co<sup>2+</sup> ions that are tetrahedrally coordinated by O<sup>2-</sup> ions on the surface might dominate the magnetism at low temperatures.<sup>5</sup> Moreover, Yan *et al.* carefully compared the temperature dependence of magnetic susceptibility and the magnetization curves of several samples with different surface morphology, that is, single crystals, a crushed powder of single crystals, and a cold pressed pellet of the powder, and they observed that crushed powder and cold pressed pellet samples, which pos-

sess relatively large surface areas, show ferromagnetism below 85 K: the ferromagnetism with  $T_c \approx 85$  K is suggested to arise from the surface of LaCoO<sub>3</sub>.<sup>10</sup> However, these arguments are based on results obtained using polycrystalline samples or particles, where the magnetism is very sensitive to a small amount of magnetic impurities and the sample morphology. Therefore, the ferromagnetism of LaCoO<sub>3</sub> is still the subject of much controversy, and direct evidence of whether the magnetism is intrinsic to the surface or an artifact is required using a LaCoO<sub>3</sub> single crystal.

In this study, we demonstrate observation of magnetic flux from a LaCoO<sub>3</sub> single-crystal surface using a scanning superconducting quantum interference device (SQUID) microscope (SSM) to reveal the ferromagnetism appearing in the LaCoO<sub>3</sub>. The observation clearly shows that the surface of the LaCoO<sub>3</sub> single crystal is ferromagnetic with a Curie temperature  $T_c \sim 85$  K. We also estimate the thickness of the ferromagnetic region using LaCoO<sub>3</sub> particle samples with various radii—these combined results give robust evidence for ferromagnetism at the surface of the LaCoO<sub>3</sub> single crystal, although XPS measurements indicate that the ferromagnetism originates from metallic behavior induced by oxygen chemisorption.

A LaCoO<sub>3</sub> single crystal was prepared by the floating zone method. Crystal growth of LaCoO<sub>3</sub> was done using polycrystalline LaCoO<sub>3</sub> prepared by solid-state reaction prior to the growth. LaCoO<sub>3</sub> particle samples were prepared in a solution process using citric acid.<sup>11</sup> La<sub>2</sub>O<sub>3</sub> was dissolved in a HNO<sub>3</sub> solution, and then an aqueous solution of Co(NO<sub>3</sub>)<sub>2</sub>·6H<sub>2</sub>O and citric acid were added and mixed thoroughly. A precursor was obtained by heating the mixture. The precursor was calcined for 12 h separately at 873, 1073, 1273, or 1473 K. Each sample calcined at a different temperature was pressed into a pellet and sintered at the same temperature. The heat treatment at different temperatures enables us to prepare particle samples with different radii. X-ray diffraction measurements were performed for the samples, and all the observed peaks could be assigned to single-phase LaCoO<sub>3</sub>: a single phase of LaCoO<sub>3</sub> can be pre-

pared even at the lowest temperature of 873 K. The oxygen content of the samples was determined using thermogravimetry, confirming no deviation from its stoichiometry for all the samples sintered at different temperatures. The particle radius was measured from scanning electron microscope images. Magnetic measurements were done using a SQUID magnetometer (Quantum Design). Stray magnetic flux from the surface of a single crystal was mapped using a SSM equipped with a pickup loop with a diameter of 10  $\mu\text{m}$  and two dc SQUIDs on a Si chip (Seiko Instruments Inc.<sup>12</sup>). A SSM can detect spatial variation of magnetic flux strayed from the surface at the ferromagnetic domain boundary with very high sensitivity.<sup>13–15</sup> To check the performance of our equipment, we also observed a single quantum flux trapped in a Nb superconductor, which was exactly  $\Phi_0=2.07 \times 10^{-7} \text{ G cm}^2$ . Prior to the measurements, the surface of the  $\text{LaCoO}_3$  single crystal was mechanically polished into optical quality in air to get flat surface morphology.

SSM images of a  $\text{LaCoO}_3$  single crystal observed in zero magnetic field in the temperature range 5–81 K are shown in Fig. 1. These images were collected from the same area of the sample. The magnetic flux distribution associated with the ferromagnetic domain structures is clearly observed at 5 and 48 K, while previous magnetic measurements on a bulk single crystal have never observed a ferromagnetic signal although a slight increase in the susceptibility was seen at low temperatures, as stated before.<sup>10</sup> The ferromagnetic signal remains faintly at 81 K and the vestige of the magnetic flux distribution is lost at 95 K, clearly showing that the surface of  $\text{LaCoO}_3$  is in a ferromagnetic state with a Curie temperature of 81–95 K.

Figure 2 shows the temperature dependences of the magnetic flux density  $B$  averaged over an  $8 \times 12 \mu\text{m}^2$  region of a single-crystal surface recorded with a SSM, accompanied with the residual magnetization  $M_r$  of a particle sample measured using a SQUID magnetometer.  $M_r$  was measured in the heating process: before the measurement, the sample was field cooled from room temperature down to 2 K under an applied magnetic field of 5 T and the field was switched off at 2 K.  $M_r$  shows an abrupt decrease with increasing temperature from 2 K and is almost constant at temperatures above 60 K, clearly different from the temperature dependence of  $B$ , with a gradual decrease up to 95 K. In general, while  $B$  measured with a SSM is sensitive in particular to stray magnetic flux just from the surface of the sample,  $M_r$  recorded using a SQUID magnetometer includes all the magnetic response from the whole sample. The different probing region depending on the measurement techniques may cause the different temperature variation in  $M_r$  and  $B$  in Fig. 2. That is, a slightly deeper portion from the sample surface, which should have a different temperature-dependent magnetization, may contribute to  $M_r$ . Similar magnetic behavior was also reported in  $\text{La}_{0.7}\text{Sr}_{0.3}\text{MnO}_3$  by J.-H. Park *et al.*<sup>16</sup> The magnetization of bulk  $\text{La}_{0.7}\text{Sr}_{0.3}\text{MnO}_3$  measured using a SQUID magnetometer showed a typical ferromagnetic temperature dependence with  $T_c \approx 360 \text{ K}$ , while samples measured with spin-resolved photoemission spectroscopy (probing depth  $\sim 5 \text{ \AA}$ ) and Mn  $L$ -edge absorption magnetic circular dichroism (probing depth  $\sim 50 \text{ \AA}$ ) exhibited different temperature dependence. From these results, the authors

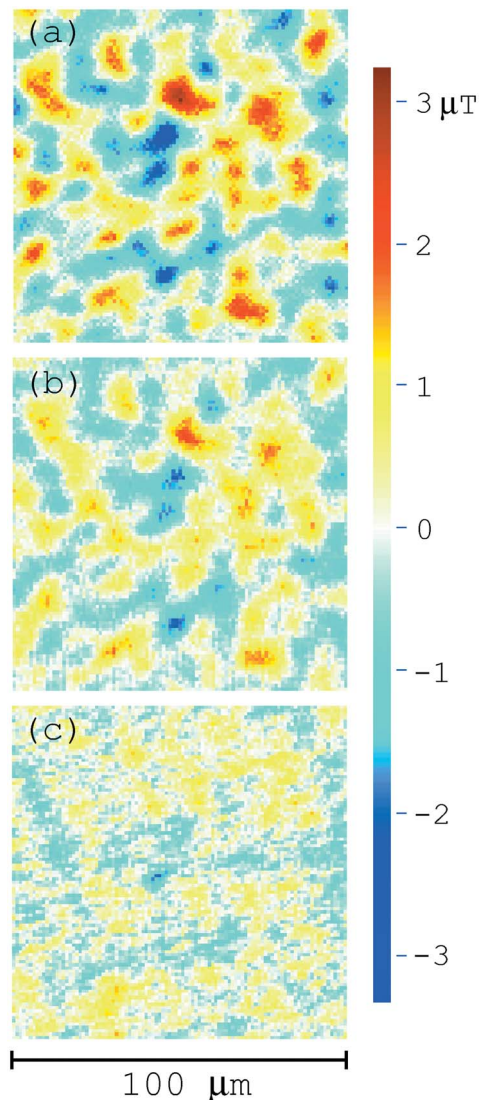


FIG. 1. (Color online) Scanning SQUID microscopy images of a  $\text{LaCoO}_3$  single crystal taken at (a) 5, (b) 48, and (c) 81 K.

concluded that at least several monolayers below the surface showed a different magnetic behavior, although the trend in magnetism is opposite to that in  $\text{LaCoO}_3$ .

In order to investigate the ferromagnetism in more detail,

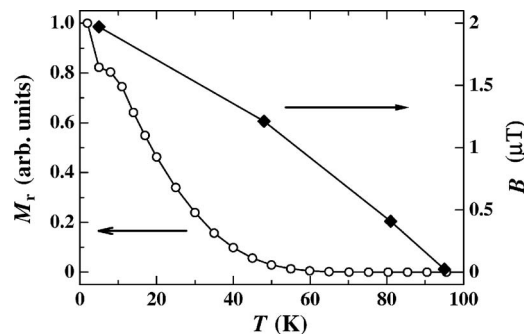


FIG. 2. Temperature dependence of magnetic flux density  $B$  and remanent magnetization  $M_r$  measured using a SSM and a SQUID magnetometer, respectively.  $M_r$  was measured for a particle sample with a particle radius of 57 nm.

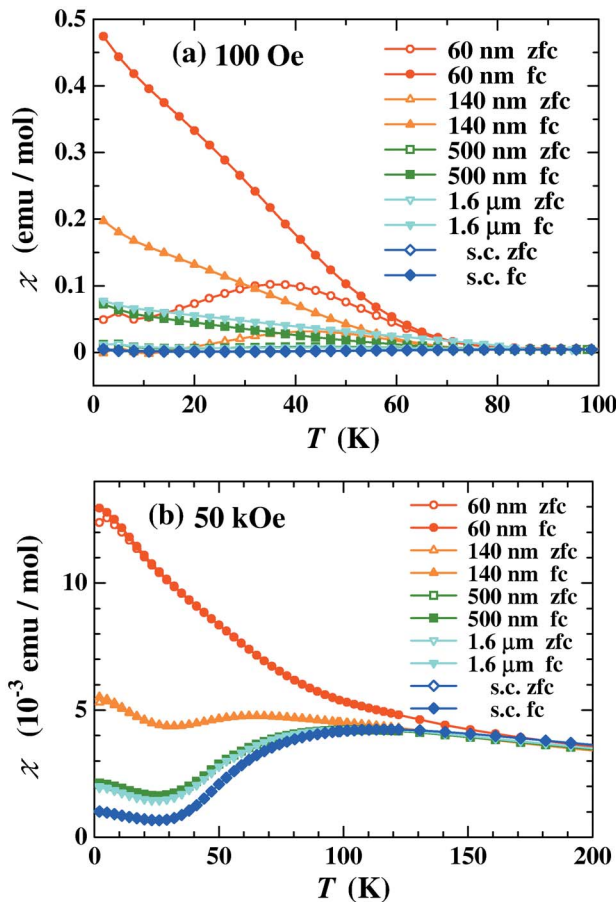


FIG. 3. (Color online) Temperature dependence of the magnetic susceptibility of LaCoO<sub>3</sub> with different particle radii measured in (a) 100 and (b) 50 kOe. “s.c.” denotes single crystal.

the magnetic behaviors of particle samples with different mean radii are compared with that of a single crystal. Since we have obtained evidence for ferromagnetism at the surface, an enhancement in the magnetization of particle samples is also likely seen, given that the particle size is reduced systematically, so that the ratio of the surface area to the volume increases. Figures 3(a) and 3(b) show the temperature-dependent magnetic susceptibilities of a single crystal and particle samples with mean radii ranging from 57 nm to 1.6 μm in 100 Oe and 50 kOe, respectively. As expected, the magnetic susceptibility becomes large as the particle size decreases. A clear bifurcation between the zero-field-cooled (ZFC) and field-cooled (FC) magnetization curves is seen for all the particle samples in 100 Oe, and the difference is largest for the smallest sample with a radius of 57 nm—see Fig. 3(a). It should also be noted that the difference between the ZFC and FC magnetization appears at a temperature between 70 and 85 K, corresponding to the Curie temperature  $T_c \sim 85$  K obtained with SSM measurements. Although a slight difference between the ZFC and FC magnetization is also observed for the single crystal, the value is quite small compared with those of the particle samples. The magnetic susceptibility in 50 kOe for the same samples is a factor of 1/36 smaller than the FC magnetic susceptibility in 100 Oe at 2 K [Fig. 3(b)], supporting the presence of ferro-

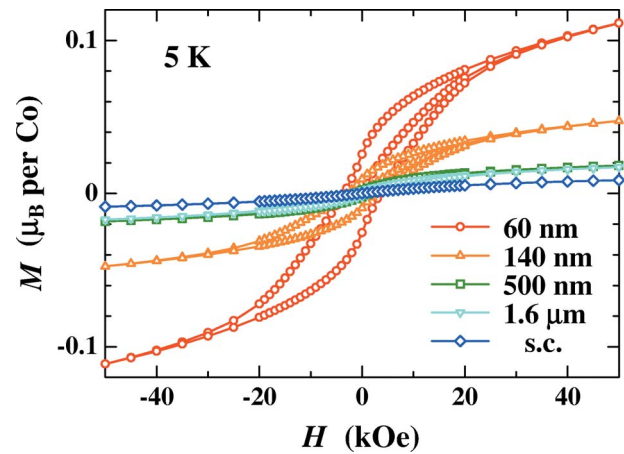


FIG. 4. (Color online) Magnetic field dependence of the magnetization of LaCoO<sub>3</sub> particle samples with different particle radii measured at 5 K. “s.c.” denotes single crystal.

magnetism with saturating magnetic behavior with increasing field.

The magnetic field  $H$  dependence of magnetization  $M$  at 5 K is shown in Fig. 4. Clear hysteresis curves appear in the particle samples, and the coercivity is becoming significant with decreasing particle size, in agreement with a previous report on LaCoO<sub>3</sub> polycrystals.<sup>10</sup> Such hysteretic behavior is less pronounced in the single crystal. These results show that the ferromagnetism we observe in LaCoO<sub>3</sub> is robust at the surface of the samples. The lack of saturation of the magnetization even in 50 kOe originates from the fact that a paramagnetic phase still exists inside the samples, as well as the ferromagnetic surface.

The electronic structure of the surface of a LaCoO<sub>3</sub> single crystal is also examined using XPS. Figure 5 shows the XPS spectra near the Fermi energy  $\epsilon_F$  (a) before and (b) after *in situ* Ar ion etching, where the feature arises mainly from O 2*p* and Co 3*d* orbitals. A significant feature is that the intensity at  $\epsilon_F$  decreases with Ar ion etching, indicating that the

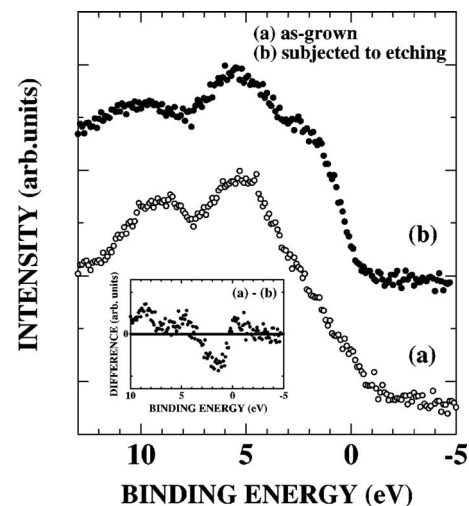


FIG. 5. XPS spectra of a LaCoO<sub>3</sub> single crystal (a) before and (b) after Ar ion etching for 5 min. Inset shows the difference between these intensities.

surface of our as-grown sample is in a metallic state and is becoming less metallic with etching. A similar metallic feature is also observed in  $\text{La}_{1-x}\text{Sr}_x\text{CoO}_3$  ( $x \geq 0.2$ ) using XPS and UPS,<sup>17,18</sup> where ferromagnetism appears due to an increase in the number of  $\text{Co}^{4+}$  ions (hole doping), on substituting  $\text{Sr}^{2+}$  for  $\text{La}^{3+}$  ions.<sup>19,20</sup> Another remarkable feature is that Ar ion etching clearly increases the intensity at around 0.5–4 eV—see Fig. 5 and the inset. Richter *et al.* reported a decrease in the XPS intensity at the same energy by exposing a sample to oxygen, and they attributed the decrease to chemisorbed oxygen.<sup>9</sup> Similarly, we infer that oxygen chemisorption occurs at the surface of our as-grown single crystal, and Ar ion etching removes the oxygen chemisorbed layer. It was also reported that a peak appeared at around 8–10 eV in UPS spectra due to chemisorbed oxygen on using HeII ( $h\nu = 40.8$  eV),<sup>9</sup> compatible with our result that a similar peak is seen in Fig. 5 for the as-grown sample. Therefore, the ferromagnetism at the surface of a  $\text{LaCoO}_3$  single crystal is likely due to the chemisorption of oxygen on the surface. From these combined results, we conclude that the ferromagnetism at the surface may originate from metallic conductivity induced by oxygen chemisorption accompanying  $\text{Co}^{4+}$  ions [hole doping; similar to the case of  $\text{La}_{1-x}\text{Sr}_x\text{CoO}_3$  ( $x \geq 0.2$ )]. However, it has also been noted that the peak at 8–10 eV observed using XPS and UPS is, apart from oxygen chemisorption, due to the adsorption of carbon monoxide  $\text{CO}$ .<sup>21</sup> Also, the overall spectral feature does not much resemble the results of XPS measurements on  $\text{LaCoO}_3$  by Saitoh *et al.*<sup>22</sup> who examined the surfaces of samples scraped *in situ*. Since we did not measure the *in situ* scraped surface, it is still inconclusive whether the ferromagnetism appears for a sample without any adsorbates.

We now estimate the thickness of the ferromagnetic region from the surface. Since the magnetization measurement using a SQUID magnetometer gives the total magnetization of a sample, the measured magnetization does not correctly represent the ferromagnetism at the surface only. Therefore, we express the measured saturation magnetization  $M_S^{\text{expt}}$  as a total of surface magnetization  $M_S$  and magnetization from the core of the particle. In the remanent state, only the ferromagnetic contribution from the surface should be included, and the expression is reduced to the following:

$$M_S^{\text{expt}} \times \frac{4}{3} \pi r^3 = M_S \times 4 \pi r^2 \Delta r,$$

where  $M_S^{\text{expt}}$  is the saturation magnetization, which averages out the ferromagnetic component over the whole particle given by extrapolating the magnetization to zero field using the data above 45 kOe in Fig. 4.  $M_S$  is the saturation magnetization of Co ions given that the surface Co ions contrib-

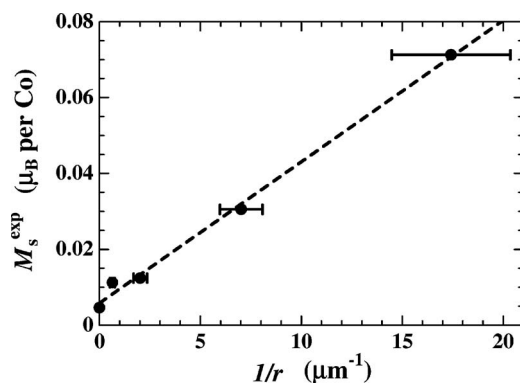


FIG. 6. Spontaneous magnetization vs  $1/r$  plot for particle samples and a single crystal using the data in Fig. 4.

ute to the magnetization,  $r$  is the radius of the particle, and  $\Delta r$  is the thickness of the ferromagnetic layer. This expression indicates that a plot of  $M_S^{\text{expt}}$  against  $1/r$  gives a straight line with a slope of  $3M_S\Delta r$ , allowing us to estimate the thickness of the surface ferromagnetic layer  $\Delta r$ . A plot of  $M_S^{\text{expt}}$  vs  $1/r$  using the data in Fig. 4 is shown in Fig. 6. The plot provides a value of  $M_S\Delta r = 1.24 \times 10^{-3} \mu\text{m} \mu_B$  per Co atom. Provided that the surface cobalt ion is in the HS  $\text{Co}^{3+}$  state ( $S=2$ ,  $M_S=4\mu_B$ ), IS  $\text{Co}^{3+}$  state ( $S=1$ ,  $M_S=2\mu_B$ ), HS  $\text{Co}^{4+}$  state ( $S=5/2$ ,  $M_S=5\mu_B$ ), IS  $\text{Co}^{4+}$  state ( $S=3/2$ ,  $M_S=3\mu_B$ ), or LS  $\text{Co}^{4+}$  state ( $S=1/2$ ,  $M_S=1\mu_B$ ), the surface thickness  $\Delta r$  is estimated to be 3.1, 6.2, 2.5, 4.1, or 12.4 Å, respectively. These values are comparable to the pseudocubic lattice parameter  $a_c = 3.803$  Å at 293 K obtained from the cell parameter of  $\text{LaCoO}_3$ .<sup>23</sup> However, if the surface magnetic moments are even as low as  $0.5\mu_B$  per Co atom as in  $\text{La}_{0.8}\text{Sr}_{0.2}\text{CoO}_3$ ,<sup>24</sup>  $\Delta r$  can be 25 Å, which corresponds to 6–7 layers of the  $\text{LaCoO}_3$  pseudocubic unit cell. Therefore, although the spin state cannot be identified, a few unit cells of the surface layers are likely ferromagnetic in any case.

In conclusion, we have reported evidence of ferromagnetism occurring at the surface of a  $\text{LaCoO}_3$  single crystal using scanning SQUID microscopy. Detailed analysis of the magnetization of  $\text{LaCoO}_3$  particle samples has allowed us to estimate the surface thickness of the ferromagnetic region to be a few unit cells of the pseudocubic lattice. XPS measurements also revealed that the ferromagnetism at the surface is presumably due to metallic conductivity induced by chemisorbed oxygen and  $\text{Co}^{4+}$  ions, indicating significant contribution of chemisorbed oxygen to the magnetism of Co oxides. Although the ferromagnetism has been clearly observed in a  $\text{LaCoO}_3$  single crystal, the predominant mechanism of the ferromagnetism is still elusive. To clarify this issue, more theoretical and experimental research is required.

\*Author to whom correspondence should be addressed. FAX: +81-45-924-5354. Email address: Mitsuru\_Itoh@msl.titech.ac.jp

<sup>1</sup>R. Pfandzelter, G. Steierl, and C. Rau, Phys. Rev. Lett. **74**, 3467 (1995).

<sup>2</sup>A. Goldoni, A. Baraldi, G. Comelli, S. Lizzit, and G. Paolucci, Phys. Rev. Lett. **82**, 3156 (1999).

<sup>3</sup>T. Shinohara, T. Sato, and T. Taniyama, Phys. Rev. Lett. **91**, 197201 (2003).

- <sup>4</sup>J. B. Goodenough, *J. Phys. Chem. Solids* **6**, 287 (1958).
- <sup>5</sup>M. A. Señarís-Rodríguez and J. B. Goodenough, *J. Solid State Chem.* **116**, 224 (1995).
- <sup>6</sup>M. A. Korotin, S. Yu. Ezhov, I. V. Solovyev, V. I. Anisimov, D. I. Khomskii, and G. A. Sawatzky, *Phys. Rev. B* **54**, 5309 (1996).
- <sup>7</sup>K. Asai, A. Yoneda, O. Yokokura, J. M. Tranquada, G. Shirane, and K. Kohn, *J. Phys. Soc. Jpn.* **67**, 290 (1998).
- <sup>8</sup>T. Kyômen, Y. Asaka, and M. Itoh, *Phys. Rev. B* **71**, 024418 (2005).
- <sup>9</sup>L. Richter, S. D. Bader, and M. B. Brodsky, *Phys. Rev. B* **22**, 3059 (1980).
- <sup>10</sup>J.-Q. Yan, J.-S. Zhou, and J. B. Goodenough, *Phys. Rev. B* **70**, 014402 (2004).
- <sup>11</sup>H. Taguchi, S. Yamada, M. Nagao, Y. Ichikawa, and K. Tabata, *Mater. Res. Bull.* **37**, 69 (2002).
- <sup>12</sup>T. Morooka, S. Nakayama, A. Odawara, M. Ikeda, S. Tanaka, and K. Chinone, *IEEE Trans. Appl. Supercond.* **9**, 3491 (1999).
- <sup>13</sup>L. N. Vu and D. J. Van Harlingen, *IEEE Trans. Appl. Supercond.* **3**, 1918 (1993).
- <sup>14</sup>J. R. Kirtley, M. B. Ketchen, K. G. Stawiasz, J. Z. Sun, W. J. Gallagher, S. H. Blanton, and S. J. Wind, *Appl. Phys. Lett.* **66**, 1138 (1995).
- <sup>15</sup>J. R. Kirtley, C. C. Tsuei, K. A. Moler, V. G. Kogan, J. R. Clem, and A. J. Turberfield, *Appl. Phys. Lett.* **74**, 4011 (1999).
- <sup>16</sup>J.-H. Park, E. Vescovo, H.-J. Kim, C. Kwon, R. Ramesh, and T. Venkatesan, *Phys. Rev. Lett.* **81**, 1953 (1998).
- <sup>17</sup>A. Chainani, M. Mathew, and D. D. Sarma, *Phys. Rev. B* **46**, 9976 (1992).
- <sup>18</sup>T. Saitoh, T. Mizokawa, A. Fujimori, M. Abbate, Y. Takeda, and M. Takano, *Phys. Rev. B* **56**, 1290 (1997).
- <sup>19</sup>M. A. Señarís-Rodríguez and J. B. Goodenough, *J. Solid State Chem.* **118**, 323 (1995).
- <sup>20</sup>S. Tsubouchi, T. Kyômen, and M. Itoh, *Phys. Rev. B* **67**, 094437 (2003).
- <sup>21</sup>P. R. Norton, J. W. Goodale, and E. B. Selkirk, *Surf. Sci.* **83**, 189 (1979).
- <sup>22</sup>T. Saitoh, T. Mizokawa, A. Fujimori, M. Abbate, Y. Takeda, and M. Takano, *Phys. Rev. B* **55**, 4257 (1997).
- <sup>23</sup>G. Thornton, B. C. Tofield, and A. W. Hewat, *J. Solid State Chem.* **61**, 301 (1986).
- <sup>24</sup>J. Okamoto, H. Miyauchi, T. Sekine, T. Shidara, T. Koide, K. Amemiya, A. Fujimori, T. Saitoh, A. Tanaka, Y. Takeda, and M. Takano, *Phys. Rev. B* **62**, 4455 (2000).